

# Blends of SAN with methyl methacrylate copolymers of 2-hydroxyethyl methacrylate and 4-methacryloxyethyl trimellitic anhydride

J.H. Chu, D.R. Paul\*

Center for Polymer Research, Department of Chemical Engineering and Texas Materials Institute, The University of Texas at Austin, Austin, TX 78712, USA

Received 14 October 1999; received in revised form 28 December 1999; accepted 28 December 1999

## Abstract

Copolymers of methyl methacrylate (MMA) with 2-hydroxyethyl methacrylate (HEMA) and 4-methacryloxyethyl trimellitic anhydride (4META) were synthesized. The miscibility regions, for blends of these copolymers with styrene–acrylonitrile (SAN) copolymers were determined. The miscibility region for MMA–HEMA copolymers is larger than that for MMA–4META copolymers. Interaction energies for monomer unit pairs were calculated from the isothermal miscibility maps using the Flory–Huggins theory combined with the binary interaction model. The experimental phase separation temperatures were found to be similar to the spinodal temperatures predicted from the lattice–fluid theory of Sanchez and Lacombe using these interaction energies. © 2000 Elsevier Science Ltd. All rights reserved.

*Keywords:* Blends; Methyl methacrylate; 2-hydroxyethyl methacrylate

## 1. Introduction

Block and graft copolymers can serve as compatibilizers that control morphology and improve the interfacial strength between phases of immiscible blends. Such copolymers can be synthesized separately and added to blends or formed in situ by reaction during processing. Reactive compatibilization can be accomplished through functional groups on polymer chains in each of the phases that can react when they meet at the interface between the two phases. This study investigates some functional monomers that may be interesting for copolymerization with methyl methacrylate (MMA) and subsequent blending with styrene–acrylonitrile copolymer (SAN). If such MMA-based copolymers are miscible with SAN, then these materials could be added in small amounts to ABS materials to be blended with polyamides, polyesters, or polycarbonates. Such functional monomers in the MMA copolymer could be envisioned to react with the condensation polymer to form in situ graft or block copolymers that locate at the domain interfaces. The objective here is to define the region of miscibility of such MMA copolymers with SAN and evaluate the relevant interaction energies.

Two monomers were investigated for use in reactive compatibilization in this study, viz. 2-hydroxyethyl

methacrylate (HEMA) and 4-methacryloxyethyl trimellitic anhydride (4META). Polymers based on HEMA have been used as a hydrogel in various medical applications [1]. One example of using HEMA as a compatibilizer has been demonstrated by Akcelrud et al. [2]. The hydroxyl groups on MMA–HEMA copolymers were reacted with the polyurethane terminal isocyanate groups to form the graft copolymer. The less familiar monomer 4META can be synthesized by reacting HEMA monomer with trimellitic anhydride chloride [3]. Copolymers of MMA and 4META have been studied and used in commercial dental applications [4–10]. Other polymer units having anhydride groups, such as maleic anhydride (MA), have been known to aid in compatibilization of blends. One possible advantage for using 4META is that it has more favorable reactivity ratios with MMA than MA, thus allowing the synthesis of more uniform copolymers. Knowledge of the miscibility regions of MMA–HEMA and MMA–4META copolymers with SAN copolymers would be helpful in further assessing the application of these units as compatibilizers.

## 2. Theory

The general thermodynamic criteria for miscibility and stability are:

$$\Delta g_{\text{mix}} = \Delta h_{\text{mix}} - T\Delta s_{\text{mix}} < 0 \quad (1)$$

\* Corresponding author. Tel.: + 1-512-471-5238; fax: + 1-512-471-7060.

E-mail address: drp@che.utexas.edu (D.R. Paul).

$$\left( \frac{\partial^2 \Delta g_{\text{mix}}}{\partial \phi_i^2} \right)_{T,P} > 0 \quad (2)$$

According to the Flory–Huggins theory [11,12] the free energy of mixing for a blend of polymers A and B is given by:

$$\Delta g_{\text{mix}} = B \phi_A \phi_B + RT \left[ \frac{\rho_A \phi_A \ln \phi_A}{M_A} + \frac{\rho_B \phi_B \ln \phi_B}{M_B} \right] \quad (3)$$

where  $R$  is the universal gas constant,  $T$  is the absolute temperature, and  $\phi_i$ ,  $\rho_i$ , and  $M_i$  are the volume fraction, density, and molecular weight of component  $i$ , respectively. The interaction energy density,  $B$ , provides information on polymer–polymer-interactions. For a miscible polymer blend,  $\Delta g_{\text{mix}}$  must be negative. The last terms of Eq. (3) are always negative and favor miscibility; however, they become smaller and smaller as the component molecular weights increase. Thus, the interaction energy density of the blend must be negative to achieve miscibility when the molecular weights become very large.

Differentiation of the Flory–Huggins expression for the free energy of mixing (Eq. (3)) gives the following expression for the interaction energy at the critical condition (Eq. (2)), where the contributions of the entropy and enthalpy of mixing are exactly balanced:

$$B_{\text{crit}} = \frac{RT}{2} \left[ \sqrt{\frac{\rho_A}{(\bar{M}_w)_A}} + \sqrt{\frac{\rho_B}{(\bar{M}_w)_B}} \right]^2 \quad (4)$$

where  $\bar{M}_w$  is the weight average molecular weight. Eq. (4) gives the value of  $B$  that sets the boundary between miscible and immiscible blends, i.e. the blend is miscible if its interaction energy is less than  $B_{\text{crit}}$  or immiscible if greater than  $B_{\text{crit}}$ . This behavior can be used in some cases to determine information about positive interaction energies.

According to the binary interaction model, [13,14] the interaction energy density of a polymer blend,  $B$ , can be expressed in terms of interactions between the various pairs of monomer units present and their volume fractions within the polymer:

$$B = \sum_{i>j} B_{ij}(\phi_i' \phi_j'' + \phi_i'' \phi_j') - \sum_{i>j} B_{ij}(\phi_i' \phi_j' + \phi_i'' \phi_j'') \quad (5)$$

where  $\phi_i'$  is the volume fraction of monomer  $i$  in copolymer A,  $\phi_j''$  is the volume fraction of monomer  $j$  in copolymer B, and  $B_{ij}$  is the interaction between monomer units  $i$  and  $j$ . For a blend of copolymer A with units 1 and 2 and copolymer B with units 3 and 4, Eq. (5) becomes:

$$B = B_{13} \phi_1' \phi_3'' + B_{14} \phi_1' \phi_4'' + B_{23} \phi_2' \phi_3'' + B_{24} \phi_2' \phi_4'' \\ - B_{12} \phi_1' \phi_2' - B_{34} \phi_3'' \phi_4'' \quad (6)$$

From Eq. (6), it can be seen that it is possible for a blend of copolymers to be miscible even though all the interaction energies are positive. Isothermal miscibility mapping in conjunction with Eq. (6) can be used to obtain information about interaction energies.

Polymer blends often exhibit phase separation on heating, or lower critical solution temperature (LCST) behavior. The Flory–Huggins theory assumes incompressibility of the polymer mixture; therefore, it is unable to predict LCST behavior in a simple way. Equation-of-state (EOS) theories, such as the lattice–fluid theory proposed by Sanchez and Lacombe, [15–19] include compressibility and naturally predict LCST behavior. The equation of state of the lattice–fluid theory is expressed in terms of reduced properties  $\tilde{P} = P/P^*$ ,  $\tilde{T} = T/T^*$ , and  $\tilde{\rho} = 1/\tilde{v} = \rho/\rho^* = v^*/v$ . The characteristic parameters are calculated by fitting experimental PVT data of the homopolymers to the lattice–fluid EOS and using mixing rules for copolymers. The characteristic pressure of the mixture  $P^*$  is related to the bare interaction energy  $\Delta P^*$ :

$$P^* = \phi_1 P_1^* + \phi_2 P_2^* - \phi_1 \phi_2 \Delta P^* \quad (7)$$

where  $P_i^*$  is the characteristic pressure of the component  $i$ . The bare interaction energy can be related to the Flory–Huggins interaction energy density at the spinodal condition as follows: [20,21]

$$B_{\text{sc}} = \tilde{\rho} \Delta P^* + \left\{ [P_2^* - P_1^* + (\phi_2 - \phi_1) \Delta P^*] \right. \\ \left. + \frac{RT}{\tilde{\rho}} \left( \frac{1}{r_1^0 v_1^*} - \frac{1}{r_2^0 v_2^*} \right) - RT \left( \frac{\ln(1 - \tilde{\rho})}{\tilde{\rho}^2} + \frac{1}{\tilde{\rho}} \right) \right. \\ \left. \times \left( \frac{1}{v_1^*} - \frac{1}{v_2^*} \right) \right\}^2 / \left\{ \frac{2RT}{v^*} \left[ \frac{2 \ln(1 - \tilde{\rho})}{\tilde{\rho}^3} \right. \right. \\ \left. \left. + \frac{1}{\tilde{\rho}^2(1 - \tilde{\rho})} + \frac{(1 - 1/r)}{\tilde{\rho}^2} \right] \right\} \quad (8)$$

Thus, by comparing experimental phase separation temperatures of the LCST type to the lattice–fluid theory, information about the interaction energy density of a blend can be obtained.

### 3. Materials and procedures

2-Hydroxyethyl methacrylate (HEMA) monomer was purified by vacuum distillation (71°C, 2 mm Hg). The middle fraction (10% top/40% bottom) was collected for further purification. The distilled HEMA monomer was then washed twice with hexanes [22]. The purity of HEMA was checked using gas chromatography. HEMA monomer was stored in the refrigerator and used within 48 h of purification. 4META was generously supplied by Sun Medical Co. of Japan and used as received. Structures of both of these monomers are shown in Fig. 1. MMA monomer was washed with an aqueous sodium hydroxide solution, rinsed with distilled water, and dried over calcium chloride or magnesium sulfate. Ethyl acrylate was dried over magnesium sulfate for the polymerizations with

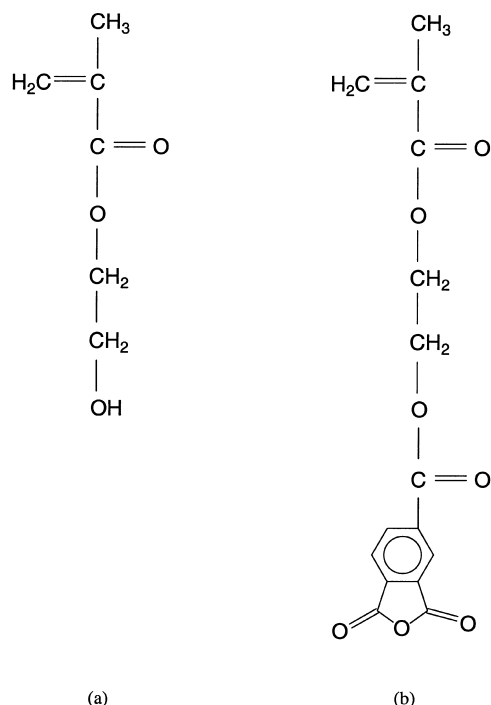


Fig. 1. Structures of monomers used in this study: (a) 2-hydroxyethyl methacrylate; (b) 4-methacryloxyethyl trimellitic anhydride.

4META. A small amount of ethyl acrylate was used in all polymerizations to prevent unzipping of the polymers. All polymerizations were performed at 60°C with AIBN as the initiator. MMA–HEMA polymers were recovered using an excess of methanol and purified using chloroform/methanol reprecipitation. MMA–4META polymers were precipitated in an excess of isopropanol and purified using chloroform/isopropanol reprecipitation. Homopolymerization of 4META was performed in dioxane dried with magnesium sulfate. The polymer was recovered by precipitation in isopropanol and purified using dioxane/isopropanol reprecipitation. Conversion was kept less than 10% to avoid composition drift in all polymers.

Fig. 2 shows plots of copolymer composition vs. reaction mass composition for the synthesized MMA–HEMA and MMA–4META copolymers. Reactivity ratios were calculated by fitting the data to the following equation:

$$F_1 = \frac{(r_1 - 1)f_1^2 + f_1}{(r_1 + r_2 - 2)f_1^2 + 2(1 - r_2)f_1 + r_2} \quad (9)$$

where  $F_1$  is the mole fraction of monomer 1 in the polymer,  $f_1$  is the mole fraction of monomer 1 in the reaction mass, and  $r_1$  and  $r_2$  are the reactivity ratios. For the polymerization of HEMA(1) with MMA(2), the reactivity ratios were found to be  $r_1 = 1.17$  and  $r_2 = 0.88$ . The reactivity ratios for copolymers of 4META(1) with MMA(2) were calculated as  $r_1 = 1.50$  and  $r_2 = 0.54$ . All copolymers synthesized in this study contain mostly MMA; the data may not be sufficient to determine reactivity ratios which represent

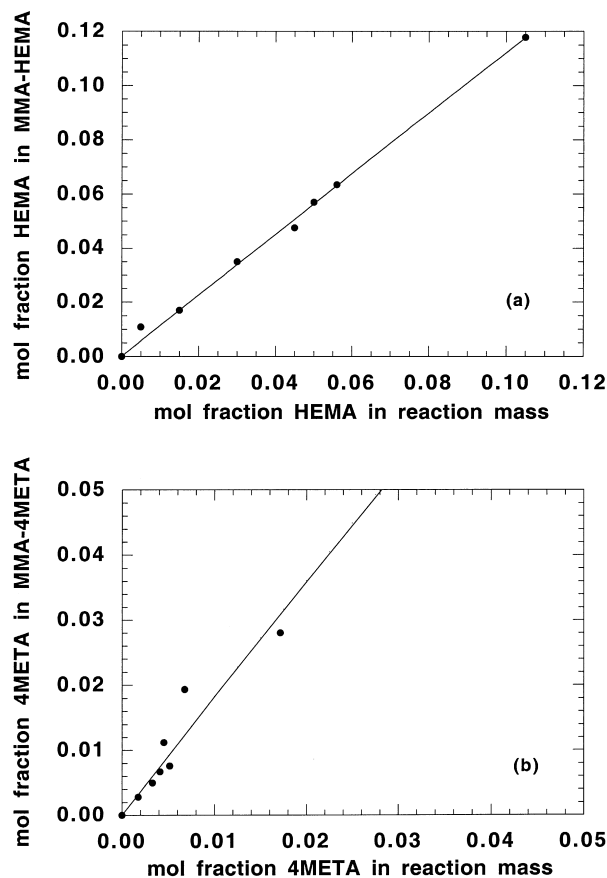


Fig. 2. Copolymer versus reaction mass composition for the free radical polymerization of MMA with: (a) 2-hydroxyethyl methacrylate; and (b) 4-methacryloxyethyl trimellitic anhydride.

the polymerization behavior over the entire composition range. However, further analysis allows for a separate determination of the  $r_2$  value in each set of reactivity ratios. Evaluating the derivative of  $F_1$ , as defined by Eq. (9), as  $f_1 \rightarrow 0$  yields:

$$\lim_{f_1 \rightarrow 0} \left( \frac{\partial F_1}{\partial f_1} \right) = \frac{1}{r_2} \quad (10)$$

Similarly, evaluating the derivative of  $F_1$  as  $f_1 \rightarrow 1$  gives:

$$\lim_{f_1 \rightarrow 1} \left( \frac{\partial F_1}{\partial f_1} \right) = \frac{1}{r_1} \quad (11)$$

Due to the compositions of the copolymers in this study, Eq. (10) is the more useful of the two derivatives for this discussion. According to Eq. (10), data close to the origin in Fig. 2 should resemble a straight line having a slope of  $1/r_2$ . The slope of the line drawn in Fig. 2a yields  $r_2 = 0.89$  for the MMA–HEMA copolymers. This is very close to the value of  $r_2 = 0.88$  found by fitting the data to Eq. (9). Similarly, the slope of the line in Fig. 2b yields  $r_2 = 0.56$  for the MMA–4META copolymers, which also is close to the value of 0.54, found using Eq. (9).

The copolymers synthesized in this study are described in Table 1. The comonomer content of these copolymers was

Table 1  
MMA copolymers synthesized for this study

| Abbreviation  | Wt% HEMA or 4META | $\bar{M}_n$ | $\bar{M}_w$ | $T_g$ (°C) |
|---------------|-------------------|-------------|-------------|------------|
| MMA–HEMA 1.4  | 1.4               | 188,800     | 451,900     | 117        |
| MMA–HEMA 2    | 2.2               | 147,600     | 370,300     | 118        |
| MMA–HEMA 4    | 4.5               | 159,400     | 414,700     | 118        |
| MMA–HEMA 6    | 6.1               | 188,800     | 475,900     | 117        |
| MMA–HEMA 7    | 7.3               | 178,600     | 451,400     | 118        |
| MMA–HEMA 8    | 8.1               | 156,500     | 444,100     | 116        |
| MMA–HEMA 15   | 14.8              | 183,100     | 424,600     | 115        |
| MMA–4META 1   | 0.8               | 180,600     | 393,700     | 119        |
| MMA–4META 1.5 | 1.5               | 143,200     | 307,900     | 115        |
| MMA–4META 2   | 2.0               | 143,900     | 340,700     | 117        |
| MMA–4META 2.3 | 2.3               | 149,300     | 358,300     | 119        |
| MMA–4META 3   | 3.3               | 71,900      | 167,900     | 117        |
| MMA–4META 5   | 5.6               | 94,900      | 199,600     | 118        |
| MMA–4META 8   | 8.0               | 91,400      | 189,600     |            |

determined by  $^1\text{H}$  NMR. Molecular weight information was obtained using gel permeation chromatography calibrated with polystyrene standards. These copolymers were blended with the various SAN copolymers, listed in Table 2. All blends containing MMA copolymers were solution cast from dichloromethane at room temperature, then dried under vacuum while increasing the temperature  $30^\circ\text{C}$  each day until  $160^\circ\text{C}$  was reached. Blends containing high molecular weight poly(2-hydroxyethyl methacrylate) (PHEMA) obtained from Aldrich were hot cast from *N,N*-dimethyl formamide (DMF) at  $90^\circ\text{C}$ , then dried under vacuum at  $160^\circ\text{C}$ . All blends cast from DMF were dried until no weight loss was detected. Blends containing high molecular weight poly(4-methacryloxyethyl trimellitic anhydride) (P4META) were cast from anhydrous THF at  $55^\circ\text{C}$ , then dried under vacuum. All polymers and blends were stored under vacuum to prevent moisture absorption.

Glass transition temperatures were determined using a Perkin–Elmer DSC-7 at a scanning rate of  $20^\circ\text{C}/\text{min}$ . A first scan was run to  $160^\circ\text{C}$  to erase thermal history and a second scan was run for analysis. Phase behavior of blends was determined using visual assessment and DSC where

Table 2  
SAN copolymers used in this study

| Polymer | Wt% AN | $\bar{M}_n$ | $\bar{M}_w$ | Source                    |
|---------|--------|-------------|-------------|---------------------------|
| SAN6.3  | 6.3    | 121,000     | 343,000     | Dow Chemical Co.          |
| SAN9.5  | 10.0   | 94,700      | 195,600     | Asahi Chemical            |
| SAN11.5 | 12.9   | 68,300      | 151,400     | Asahi Chemical            |
| SAN13.5 | 15.2   | 56,300      | 149,000     | Asahi Chemical            |
| SAN15.5 | 17.7   | 65,300      | 144,300     | Asahi Chemical            |
| SAN20   | 20     | 88,000      | 178,700     | Dow Chemical Co.          |
| SAN23   | 23     | 43,300      | 117,500     | Daicel Chemical ind. Ltd. |
| SAN25   | 25     | 77,000      | 152,000     | Dow Chemical Co.          |
| SAN27   | 26.9   | 57,000      | 142,000     | Monsanto                  |
| SAN28   | 28.4   | 52,900      | 143,800     | Asahi Chemical            |
| SAN30   | 30     | 81,000      | 168,000     | Dow Chemical Co.          |
| SAN33   | 33     | 68,000      | 146,000     | Monsanto Co.              |

possible. Phase separation temperatures were determined using a Mettler FP82HT Hot Stage equipped with a Mettler FP80HT Central Processor. A Gnomix PVT apparatus was used to obtain PVT data for PHEMA from which the characteristic Sanchez–Lacombe EOS parameters were calculated.

#### 4. MMA–HEMA/SAN blends

The isothermal miscibility map for blends of methyl methacrylate–2-hydroxyethyl methacrylate (MMA–HEMA) copolymers with styrene–acrylonitrile (SAN) copolymers is shown in Fig. 3, where the open circles represent miscible blends and the filled circles represent immiscible blends. The region of miscibility is a closed loop with the greatest range of miscibility being for pure PMMA. Miscibility of pure PMMA is observed with SAN copolymers containing between 12.9 wt% AN and 30 wt% AN as found previously [23–29]. The addition of HEMA to the MMA polymers causes the AN limits to narrow and eventually vanish. MMA–HEMA copolymers containing up to 7.3 wt% HEMA exhibited some miscibility with SAN copolymers, but those having 8.1 wt% HEMA or greater were immiscible with all SAN copolymers. Blends of PHEMA homopolymer with SAN copolymers were also immiscible (not shown in Fig. 3). It was found previously that poly(ethyl methacrylate) is miscible with all SAN copolymers having less than 28–30 wt% AN including polystyrene homopolymer [24,30]. The only structural difference between ethyl methacrylate and HEMA is the hydroxyl group on the terminal alkyl group. Thus, the addition of this hydroxyl group causes immiscibility with PS homopolymer and a wide range of SAN copolymers.

As seen from Eq. (6), six interaction energies are necessary to describe this blend system:  $B_{S/\text{MMA}}$ ,  $B_{\text{MMA}/\text{AN}}$ ,  $B_{S/\text{AN}}$ ,  $B_{\text{MMA}/\text{HEMA}}$ ,  $B_{S/\text{HEMA}}$ , and  $B_{\text{HEMA}/\text{AN}}$ . Three of these

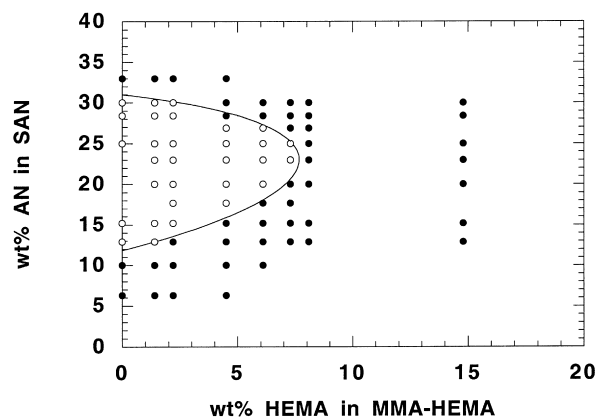


Fig. 3. Isothermal miscibility map at  $160^\circ\text{C}$  for 50/50 wt% blends of MMA–HEMA copolymers with SAN copolymers: (○) miscible; (●) immiscible. The solid curve was calculated from the  $B_{ij}$  set obtained from the best fit of the miscibility map:  $B_{\text{MMA}/\text{HEMA}} = 1.81$ ,  $B_{S/\text{MMA}} = 0.22$ ,  $B_{\text{MMA}/\text{AN}} = 4.48$ ,  $B_{S/\text{HEMA}} = 3.11$ ,  $B_{\text{HEMA}/\text{AN}} = 4.86$ , and  $B_{S/\text{AN}} = 6.99 \text{ cal}/\text{cm}^3$ .

Table 3  
Polymer standards used in this study

| Polymer     | $\bar{M}_n$ | $\bar{M}_w/\bar{M}_n$ | Source               |
|-------------|-------------|-----------------------|----------------------|
| PS 580      | 580         | 1.18                  | Polymer Laboratories |
| PS 680      | 680         | 1.16                  | Polymer Laboratories |
| PS 800      | 800         | 1.30                  | Pressure Chemical    |
| PS 1350     | 1350        | 1.07                  | Polymer Laboratories |
| PS 2000     | 2000        | 1.06                  | Pressure Chemical    |
| PS 4000     | 4000        | < 1.06                | Pressure Chemical    |
| PS 9200     | 9200        | 1.03                  | Polymer Laboratories |
| PS 17,500   | 17,500      | 1.04                  | Pressure Chemical    |
| PS 22,000   | 22,000      | 1.03                  | Polymer Laboratories |
| PS 100,000  | 100,000     | < 1.06                | Pressure Chemical    |
| PMMA 1210   | 1210        | 1.16                  | Polymer Laboratories |
| PMMA 1400   | 1400        | 1.16                  | Polymer Laboratories |
| PMMA 2400   | 2400        | 1.08                  | Polymer Laboratories |
| PMMA 4250   | 4250        | 1.07                  | Polymer Laboratories |
| PMMA 5720   | 5720        | 1.06                  | Polymer Laboratories |
| PMMA 10,550 | 10,550      | 1.11                  | Polymer Laboratories |
| PMMA 13,000 | 13,000      | 1.03                  | Polymer Laboratories |
| PMMA 20,300 | 20,300      | 1.11                  | Polymer Laboratories |

interaction energies have been evaluated previously in other studies:  $B_{S/MMA} = 0.18 - 0.26 \text{ cal/cm}^3$  [31–38],  $B_{MMA/AN} = 4.1 - 4.55 \text{ cal/cm}^3$ , [28,36,38,39] and  $B_{S/AN} = 6.7 - 8.0 \text{ cal/cm}^3$  [28,29,35–38,40]. In an attempt to obtain some information regarding the other interaction energies, high molecular weight PHEMA homopolymer was blended with PS and PMMA homopolymers of various molecular weights. Table 3 provides information about the polymer standards used in these experiments. All blends of PHEMA homopolymer with PS homopolymers, ranging in molecular weight from 22,000 to 580, were immiscible; thus  $B_{S/HEMA} > 0.73 \text{ cal/cm}^3$ . Similarly, all blends of PHEMA homopolymer with PMMA homopolymers of molecular weights between 20,300 and 1210 were immiscible, so  $B_{MMA/HEMA} > 0.41 \text{ cal/cm}^3$ . Blends of MMA–HEMA 15 with PMMA homopolymers were evaluated to obtain an upper limit for the MMA/HEMA interaction energy. Due to the closeness of the refractive indices and glass transition temperatures of these polymers, miscibility could be evaluated only for blends with PMMA homopolymers having a molecular weight of 4250 or less. All of these blends were found to be miscible, so  $0.41 < B_{MMA/HEMA} <$

Table 4  
Interaction energies from this study ( $\text{cal/cm}^3$ )

| Interaction pair | MMA–HEMA/SAN    | MMA–4META/SAN   |
|------------------|-----------------|-----------------|
| S/MMA            | 0.22            | 0.22            |
| MMA/AN           | $4.48 \pm 0.03$ | $4.48 \pm 0.01$ |
| S/AN             | $6.99 \pm 0.04$ | $6.99 \pm 0.01$ |
| MMA/HEMA         | $1.81 \pm 0.10$ | –               |
| MMA/4META        | –               | $3.84 \pm 0.10$ |
| S/HEMA           | $3.11 \pm 0.11$ | –               |
| S/4META          | –               | $7.68 \pm 0.08$ |
| HEMA/AN          | $4.86 \pm 0.26$ | –               |
| 4META/AN         | –               | $6.18 \pm 0.08$ |

$4.89 \text{ cal/cm}^3$ . Since the necessary polyacrylonitrile polymers are not available, this approach could not be used to obtain information about  $B_{HEMA/AN}$ .

A computer program, described elsewhere [41], was used to determine the set of interaction energies, as defined by theory and constrained by the previously determined range of possible values, that best fit the experimental data. The best fit to the data is shown by the curve in Fig. 3. The interaction energies defining this curve are listed in Table 4. The confidence limits for the calculated interaction energies, found by adjusting each interaction parameter and determining the limit where a fit to the miscibility data could be found by changing the other parameters [42], are also given in Table 4. From the miscibility information, the three interaction energies with HEMA are  $B_{MMA/HEMA} = 1.81 \pm 0.10$ ,  $B_{S/HEMA} = 3.11 \pm 0.11$ , and  $B_{HEMA/AN} = 4.86 \pm 0.26 \text{ cal/cm}^3$ . The values found for the other three interaction energies are consistent with values found elsewhere at similar temperatures [39].

Four MMA–HEMA blends with SAN were found to exhibit LCST behavior; the blends and the corresponding phase separation temperatures are listed in Table 5. In order to compare the LCST behavior to the interaction energies found with the miscibility map, experimental PVT data for PHEMA were obtained as described earlier; the lattice–fluid theory characteristic parameters deduced from these data for the temperature range 150–180°C are  $P^* = 597.3 \text{ MPa}$ ,  $T^* = 684 \text{ K}$  and  $\rho^* = 1.0862 \text{ g/cm}^3$ . Using the Flory–Huggins interaction energies determined from the copolymer miscibility map and the appropriate characteristic parameters with the lattice–fluid theory, the lattice–fluid interaction energies were calculated via Eq. (8). The latter were then used to predict the spinodal temperatures shown in Table 5. While the experimental phase separation temperatures do not necessarily correspond to the spinodal temperatures, they are expected to follow a similar trend. As seen by comparing the values given in Table 5, the experimental phase separation temperatures and calculated spinodal temperatures are indeed similar.

## 5. MMA–4META/SAN blends

Blends of (methyl methacrylate–4-methacryloxyethyl trimellitic anhydride) MMA–4META copolymers with SAN copolymers were cast and the miscibility data are shown in Fig. 4. As with the MMA–HEMA copolymer blends, the greatest range of miscibility with SAN copolymers is observed with pure PMMA. The region of miscibility has a shape similar to that for MMA–HEMA/SAN blends, but encompasses a smaller area. MMA–4META copolymers containing up to 2.3 wt% 4META were miscible with some SAN copolymers, however those having 3.3 wt% 4META or greater were immiscible with all SAN copolymers. As seen by comparing Figs. 3 and 4, the addition of the trimellitic anhydride group onto the

Table 5  
Predicted spinodal temperatures and experimental phase separation temperatures for blends in this study

| Blend (50/50 wt%)     | Predicted spinodal temperature (°C) | Experimental phase separation temperature (°C) |
|-----------------------|-------------------------------------|--|
| MMA–HEMA 1.4/SAN 28.4 | 204                                 | 180–185  |
| MMA–HEMA 1.4/SAN30    | 150                                 | 160–170  |
| MMA–HEMA 2/SAN28.4    | 191                                 | 210–220  |
| MMA–HEMA 2/SAN30      | 141                                 | 170–175  |

HEMA monomer unit to create the 4META unit significantly decreases the miscibility of the MMA copolymers with SAN copolymers. This shows a limitation to the amount of functionality that can be incorporated into a miscible blend; up to 5.7 mol% HEMA can be used in MMA copolymers and obtain a miscible blend with SAN where as only up to 0.8 mol% 4META can be used. None of the MMA–4META/SAN blends exhibited LCST/UCST behavior.

Again, six interaction energies are needed for this blend system, of which three,  $B_{S/MMA}$ ,  $B_{MMA/AN}$ , and  $B_{S/AN}$ , have been discussed earlier. High molecular weight P4META homopolymer was blended with PS and PMMA homopolymers of various molecular weights to gain information regarding  $B_{S/4META}$  and  $B_{MMA/4META}$ ; as discussed earlier polyacrylonitrile polymers are not available for this type of study. Since all blends of P4META homopolymer with PS homopolymers, ranging in molecular weight from 100,000 to 800, were immiscible,  $B_{S/4META} > 0.44 \text{ cal/cm}^3$ . Similarly, all blends of P4META homopolymer with PMMA homopolymers of molecular weights between 20,300 and 1210 were immiscible, so  $B_{MMA/4META} > 0.33 \text{ cal/cm}^3$ . Blends of MMA–4META with PMMA homopolymers were evaluated to gather

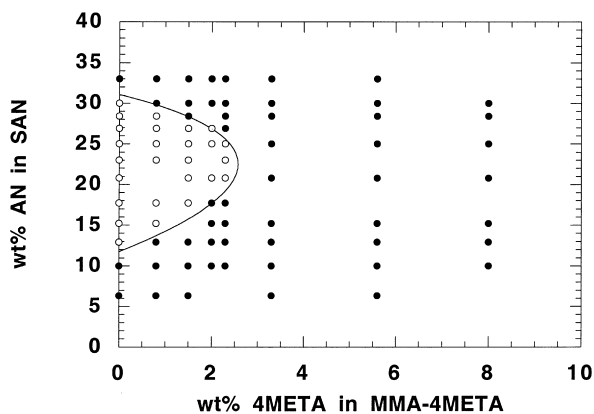


Fig. 4. Isothermal miscibility map at 160°C for 50/50 wt% blends of MMA–4META copolymers with SAN copolymers: (○) miscible; (●) immiscible. The solid curve was calculated from the  $B_{ij}$  set obtained from the best fit of the miscibility map:  $B_{MMA/4META} = 3.84$ ,  $B_{S/MMA} = 0.22$ ,  $B_{MMA/AN} = 4.48$ ,  $B_{S/4META} = 7.68$ ,  $B_{4META/AN} = 6.18$ , and  $B_{S/AN} = 6.99 \text{ cal/cm}^3$ .

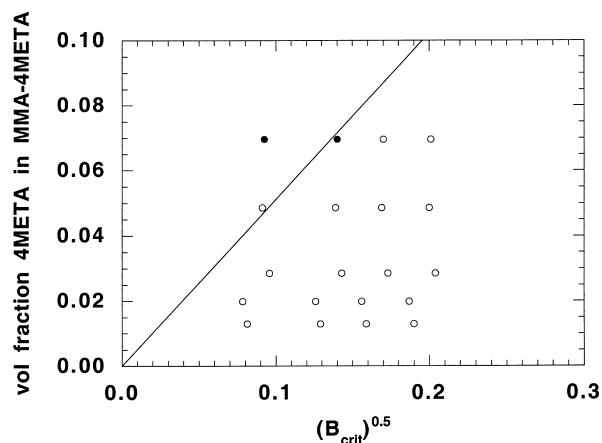


Fig. 5. Isothermal miscibility map for 50/50 blends of MMA–4META copolymers with PMMA homopolymers of varying molecular weights plotted according to Eq. (13): (○) miscible; (●) immiscible.

more information about the MMA/4META interaction energy. The form of Eq. (5) applicable to blends of MMA–4META/PMMA is:

$$B = B_{MMA/4META} \phi_{4META}'' \quad (12)$$

Combining Eqs. (4) and (12) leads to:

$$\phi_{4META}'' = \sqrt{\frac{B_{crit}}{B_{MMA/4META}}} \quad (13)$$

Thus, a plot of the data in the form of  $\phi_{4META}''$  versus  $\sqrt{B_{crit}}$  can be used to generate a straight line that will separate the miscible and immiscible blends. This line, which must pass through the origin, has a slope of  $1/\sqrt{B_{MMA/4META}}$ . Fig. 5 shows the data for MMA–4META/PMMA blends plotted in this manner. Only two of these blends were found to be immiscible, all others were miscible. A line from the origin was drawn that would best fit the data to obtain a first guess for the interaction energy. Using the slope of that line in conjunction with Eq. (13) leads to the estimation of  $B_{MMA/4META} = 3.84 \text{ cal/cm}^3$ .

Using all of this miscibility data, a set of interaction energies that best fit the MMA–4META/SAN miscibility map was determined. These interaction energies are represented by the curve shown in Fig. 4. The relevant interaction energies along with their confidence limits are given in Table 4. The three interaction energies with 4META were determined to be  $B_{MMA/4META} = 3.84 \pm 0.10$ ,  $B_{S/4META} = 7.68 \pm 0.08$ , and  $B_{4META/AN} = 6.18 \pm 0.08 \text{ cal/cm}^3$ .

It is interesting to compare the interaction energies of ethyl methacrylate (EMA), HEMA, and 4META with styrene. It has been reported that  $B_{S/EMA} = -0.0361 \text{ cal/cm}^3$  [30]. Thus, the addition of the hydroxyl group onto EMA to form HEMA causes the interaction energy to change from a slightly negative to a quite positive value. The interaction energy of styrene with 4META is larger than both of these, suggesting interaction of styrene is more unfavorable with

4META than HEMA and EMA, even though they both contain an aromatic ring.

## 6. Summary

Copolymers of MMA with HEMA and 4META were synthesized and characterized. The miscibility regions for SAN copolymers with MMA–HEMA and MMA–4META copolymers were determined. The miscibility window was the largest with PMMA and closed entirely with MMA–HEMA copolymers containing 8.1 wt% HEMA and greater, and with MMA–4META copolymers containing 3.3 wt% 4META and greater. The miscibility data were used in conjunction with the Flory–Huggins theory and the binary interaction model to calculate interaction energies. All interaction energies determined in this study are positive, as seen in Table 4; the three interaction energies studied previously are consistent with values found in the literature. Only a few blends of MMA–HEMA with SAN were found to exhibit phase separation on heating. The phase separation temperatures were similar to the spinodal temperatures predicted using the lattice–fluid theory and the binary interaction energies.

## Acknowledgements

The authors wish to thank Dr C. Grant Willson and his research group for their assistance in this project. This research was funded by National Science Foundation grant numbers DMR 92-15926 and DMR 97-26484 administered by the Division of Materials Research-Polymers Program.

## References

- [1] Ratner BD, Hoffman AS. In: Andrade JD, editor. *Hydrogels for medical and related applications*, vol. 31. Washington, DC: American Chemical Society, 1976.
- [2] Akcelrud L, Gomes AS. *J Polym Sci: Polym Chem* 1986;24:2831.
- [3] Takeyama M, Kashibuchi S, Nakabayashi N, Masuhara EJ. *Jpn Soc Dent Appar Mater* 1978;19:179.
- [4] Masuhara E, Nakabayashi N, Takeyama M. US Patent 4,148,988, Mitsui Petrochemical Industries Ltd., 1979.
- [5] Nakabayashi N, Kojima K, Masuhara EJ. *Biomed Mater Res* 1982;16:265.
- [6] Ishihara K, Nakabayashi NJ. *Biomed Mater Res* 1989;23:1475.
- [7] Inoue T, Shimono M. *Proc Finn Dent Soc* 1992;88(Suppl 1):183.
- [8] Suzuki S, Sakoh M, Shiba A. *J Biomed Mater Res* 1990;24:1091.
- [9] Suzuki M, Kato H, Wakumoto S. *J Dent Res* 1991;70:1092.
- [10] Suzuki S, Cox CF, White KC. *Quintessence Int* 1994;25:477.
- [11] Flory PJ. *J Chem Phys* 1942;10:51.
- [12] Huggins ML. *J Chem Phys* 1941;9:440.
- [13] Paul DR, Barlow JW. *Polymer* 1984;25:487.
- [14] Paul DR. *Pure Appl Chem* 1995;67:977.
- [15] Lacombe RH, Sanchez IC. *J Phys Chem* 1976;80:2568.
- [16] Sanchez IC, Lacombe RH. *J Phys Chem* 1976;80:2353.
- [17] Sanchez IC, Lacombe RH. *Polym Sci: Polym Lett* 1977;15:71.
- [18] Sanchez IC, Lacombe RH. *Macromolecules* 1978;11:1145.
- [19] Sanchez IC. In: Meyers RA, editor. *Encyclopedia of physical science and technology*, vol. 11. New York: Academic Press, 1987.
- [20] Kim CK, Paul DR. *Polymer* 1992;33:1630.
- [21] Callaghan TA. PhD dissertation, The University of Texas at Austin, 1992.
- [22] Stevenson WTK, Evangelista RA, Broughton RL, Sefton MV. *J Appl Polym Sci* 1987;34:65.
- [23] Chiou JS, Paul DR, Barlow JW. *Polymer* 1982;23:1543.
- [24] Fowler ME, Barlow JW, Paul DR. *Polymer* 1987;28:1177.
- [25] Cowie JMG, Lath D. *Makromol Chem Macromol Symp* 1988;16:103.
- [26] Suess J, Kressler J, Kammer HW. *Polymer* 1987;28:957.
- [27] Kressler J, Kammer HW, Klostermann K. *Polym Bull* 1986;15:113.
- [28] Nishimoto M, Keskkula H, Paul DR. *Polymer* 1989;30:1279.
- [29] Nishimoto M, Keskkula H, Paul DR. *Macromolecules* 1990;23:3633.
- [30] Brannock GR, Barlow JW, Paul DR. *J Polym Sci: Polym Phys* 1991;29:413.
- [31] Callaghan TA, Paul DR. *Macromolecules* 1993;28:2439.
- [32] Fukuda T, Inagaki H. *Pure Appl Chem* 1983;55:1541.
- [33] Fukuda T, Nagata M, Inagaki H. *Macromolecules* 1984;17:548.
- [34] Fukuda T, Nagata M, Inagaki H. *Macromolecules* 1986;19:1411.
- [35] Gan PP, Paul DR. *Polymer* 1994;35:3513.
- [36] Gan PP, Paul DR. *Polymer* 1994;35:1487.
- [37] Gan PP, Paul DR. *J Appl Polym Sci* 1994;54:317.
- [38] Nishimoto M, Takami Y, Tohara A, Kasahara H. *Polymer* 1995;36:1441.
- [39] Chu JH, Paul DR. *Polymer* 1999;40:2687.
- [40] Keitz JD, Barlow JW, Paul DR. *J Appl Polym Sci* 1984;29:3131.
- [41] Chu JH. PhD dissertation, The University of Texas at Austin, 1999.
- [42] Merfeld GD, Paul DR. *Polymer* 1998;39:1999.